



Universiteit  
Leiden  
The Netherlands

## Scaling limits in algebra, geometry, and probability

Arzhakova, E.

### Citation

Arzhakova, E. (2022, February 23). *Scaling limits in algebra, geometry, and probability*. Retrieved from <https://hdl.handle.net/1887/3276037>

Version: Publisher's Version

License: [Licence agreement concerning inclusion of doctoral thesis in the Institutional Repository of the University of Leiden](#)

Downloaded from: <https://hdl.handle.net/1887/3276037>

**Note:** To cite this publication please use the final published version (if applicable).

## Chapter 6

# Connectivity of real isoperiodic sets on a torus with 3 poles<sup>1</sup>

### 6.1 Introduction

A Riemann surface is a connected manifold of complex dimension one that is equipped with a complex structure, i.e., with an atlas of open charts  $\{U_i\}$  and a collection of homeomorphisms to the open disk  $f_i: U_i \rightarrow D \subset \mathbb{C}$ ; the transition functions  $g_{ij}$  between the charts  $U_i$  and  $U_j$  are given by the equality  $f_i = g_{ij} \circ f_j$ . The transition maps are required to be holomorphic, i.e., differentiable at any point of their domain. Any open set in  $\mathbb{C}$  is naturally a Riemann surface; some of the examples include the unit disk  $\mathbb{D} = \{z: |z| < 1\}$  and the upper half-plane  $\mathbb{H} = \{z \in \mathbb{C}: \text{Im}z > 0\}$ . The simplest example of a compact Riemann surface is the sphere  $\widehat{\mathbb{C}} = \mathbb{C} \cup \{\infty\}$  with charts  $U_1 = \mathbb{C}$  and  $U_2 = \widehat{\mathbb{C}} - \{0\}$  and homeomorphisms  $f_1 = z$  and  $f_2 = 1/z$ . Then, both transition maps  $g_{1,2}$  and  $g_{2,1}$  are given by a holomorphic function  $z \mapsto 1/z$ . By the classification theorem, any orientable compact surface  $X$  is homeomorphic to either a sphere  $\widehat{\mathbb{C}}$  or a  $g$ -holed torus with  $g \geq 1$  [27]. The number  $g$  is called the genus of the surface. For some applications it is important to consider pointed Riemann surfaces, i.e., the data of the Riemann surface with a finite number of points on it.

It is convenient to consider Riemann surfaces with fixed genus  $g$  and fixed number of marked points as elements of some space. There are many choices of such spaces, the most notable ones include the Teichmüller space and

---

<sup>1</sup>This chapter is based on: E. Arzhakova, G. Calsamiglia, B. Deroin, Isoperiodic moduli spaces of meromorphic forms, in progress

the moduli space.

- The Teichmuller space. Fix a reference surface – an oriented closed surface  $S$  of genus  $g$  with  $n \geq 0$  ordered distinct marked points. The Teichmuller space  $T(S)$  associated to  $S$  is a space of equivalence classes of pairs  $(X, f)$  where  $X$  is a Riemann surface with  $n$  ordered distinct marked points and  $f: S \rightarrow X$  is a diffeomorphism between the surfaces that maps the ordered marked points of  $S$  to the ordered marked points of  $X$ . The equivalence in  $T(S)$  is described as follows: two pairs  $(X_1, f_1)$  and  $(X_2, f_2)$  are equivalent if  $f_1 \circ f_2^{-1}: X_2 \rightarrow X_1$  is isotopic to a holomorphic diffeomorphism. The Teichmuller space is connected and has a canonical complex manifold structure [3, 8].

**Example 6.1.1** (Teichmuller space of a torus). Consider the reference surface to be a torus  $\mathbb{T} = \mathbb{R}^2/\mathbb{Z}^2$ . Any complex structure on a torus can be realised by a Riemann surface of a form  $\mathbb{C}/(\mathbb{Z} + \tau\mathbb{Z})$  where  $\tau \in \mathbb{C}$  is such that  $\text{Im}\tau > 0$ . Note that such complex numbers form an upper half-plane  $\mathbb{H} = \{z \in \mathbb{C} : \text{Im}z > 0\}$ . The map  $\mathbb{H} \rightarrow T(\mathbb{T})$  given by  $\tau \mapsto \mathbb{C}/\langle 1, \tau \rangle$  is a bijection and, therefore,  $T(\mathbb{T}) = \mathbb{H}$ .

- The moduli space. The mapping class group  $\text{Mod}(S)$  of a surface  $S$  is the group of isotopy classes of homeomorphisms of  $S$  that fix each marked point. In other words,  $\text{Mod}(S) = \text{Homeo}(S)/\text{Homeo}_0(S)$  where  $\text{Homeo}_0(S)$  are the homeomorphisms isotopic to identity. The moduli space  $\mathcal{M}_S$  is given by the quotient  $T(S)/\text{Mod}(S)$ . In fact, the moduli space depends only on the genus  $g$  and number of marked points  $n$  of the surface  $S$ , therefore, it is usually denoted as  $\mathcal{M}_{g,n}$ . The moduli space has an orbifold structure, it is typically not a manifold.

**Example 6.1.2** (Moduli space of a torus). The mapping class group of a torus  $\text{Mod}(\mathbb{T})$  is isomorphic to  $SL(2, \mathbb{Z})$ . It follows that  $\mathcal{M}_{1,0} = \mathbb{H}/SL(2, \mathbb{Z})$ .

Differential forms can be defined on the Riemann surfaces, in particular, the space of the 1-forms is the dual vector space to the tangent space of a surface. In a local coordinate  $z$  given by the complex structure a differential 1-form can be written as  $\omega = f(z) dz$ .

- A 1-form  $\omega$  on a surface  $X$  is called a *holomorphic differential* if  $f(z)$  is holomorphic, i.e., a complex differentiable function. Denote by  $N$  the set of zeroes of  $\omega$ ;  $N = \{x \in X : \omega(x) = 0\}$ . Then,  $X \setminus N$  inherits a flat

metric and in the neighbourhood of a zero this metric admits a conical singularity of angle  $2\pi(k+1)$ . In other words, in the neighborhood of a zero the 1-form  $\omega$  is locally given by  $z^k dz$ ,  $k \geq 1$ . In this case, we say that  $k$  is the order of the zero. The flat metric defined locally by a zero of order  $k$  is a ramified covering over a flat disk of order  $k+1$  that is ramified at zero.

- A 1-form  $\omega$  on a surface  $X$  is called a *meromorphic differential* if  $f(z)$  is a meromorphic function. i.e., it is holomorphic everywhere except in a discrete set of points that are called the poles of the function. Locally at the pole  $\omega = z^{-k} dz$  and  $k$  is the order of the pole. The singularities of a pair  $(X, \omega)$  consist of poles and zeroes; let us define the degree of a singularity to be  $k$  if it is a zero of order  $k$ , and  $-k$  if it is a pole of order  $k$ . Denote by  $n_i$  the degree of the  $i$ -th singularity of  $X$ ; then, as a consequence of the Riemann-Roch theorem, we obtain that  $\sum n_i = 2g - 2$  [102].

Select a pole on  $X$  and denote it by  $p$ . Choose a short closed curve  $\gamma_p$  going around  $p$ , i.e., a curve that has no other singularity in its interior and does not wind around genus. The complex number  $\text{res}_p(\omega) = \frac{1}{2\pi i} \int_{\gamma_p} \omega$  is called the residue of the form  $\omega$  at  $p$  and it does not depend on the choice of  $\gamma_p$ . Let  $(X, \omega)$  be a Riemann surface with poles  $p_1, \dots, p_n$ . Then, by the residue theorem,  $\sum_1^n \text{res}_p(\omega) = 0$  [102].

Consider a closed curve  $c$  on a Riemann surface  $X$  and introduce a 1-form  $\nu_c$  such that for every closed 1-form  $\alpha$ ,  $\int_c \alpha = -\int \alpha \wedge \nu_c = (\alpha, \star \nu_c)$  where  $\star$  is the Hodge star. Then, we define an intersection of two closed curves  $a$  and  $b$  on  $X$  as  $a \cdot b = \int \nu_a \wedge \nu_b$ . The intersection form is an anti-symmetric form with its image contained in  $\mathbb{Z}$  and the intersection of  $a$  and  $b$  depends only on the homology classes of  $a$  and  $b$ . Denote a surface of genus  $g$  with  $n$  poles as  $\Sigma_{g,n}$ . The intersection form enables us to select a basis of the fundamental group  $\pi_1(\Sigma_{g,n})$  given by  $\{a_1, b_1, \dots, a_g, b_g, \pi_1, \dots, \pi_n\}$  such that  $a_i \cdot b_j = \delta_{i,j}$ ,  $a_i \cdot \pi_j = b_i \cdot \pi_j = \pi \cdot \pi_j = 0$ .

In the follow-up we are interested in comparing integrals of 1-forms over a basis of  $H_1(X, \mathbb{Z})$ . Therefore, it is natural to seek some space of Riemann surfaces that identifies the curves in  $H_1(X, \mathbb{Z})$  for different  $X$ . The most convenient space for this goal is the Torelli space and it is defined as follows. Denote by  $\Sigma_{g,n^*}$  a surface obtained by making punctures at each marked point of  $\Sigma_{g,n}$ , i.e.,  $\Sigma_{g,n^*} = \Sigma_{g,n} \setminus N$  where  $N$  is the set of  $n$  marked points. The subgroup  $\mathcal{I}_{g,n}$  of  $\text{Mod}(\Sigma_{g,n})$  that acts trivially on  $H_1(\Sigma_{g,n^*})$  is called the

Torelli group of  $\Sigma_{g,n^*}$ . The Torelli space  $\mathcal{S}_{g,n}$  is given by  $T_{g,n}/\mathcal{I}_{g,n}$  and the pullback of the 1-form bundle  $\Omega\mathcal{M}_{g,n}$  over the moduli space by the cover  $\mathcal{S}_{g,n^*} \rightarrow \mathcal{M}_{g,n}$  is denoted by  $\Omega\mathcal{S}_{g,n^*}$ . A point in  $\Omega\mathcal{S}_{g,n^*}$  is therefore described by a fourtuple  $(X, N, [f], \omega)$  where  $[f]$  is the equivalence class of the homotopical collapse map  $f$  under the action of the Torelli group.

**Definition 6.1.3.** The map  $\text{Per}_{g,n} : \Omega\mathcal{S}_{g,n} \rightarrow \text{Hom}(H_1(\Sigma_{g,n^*}, \mathbb{C}))$  is defined by the formula

$$\text{Per}_{g,n}(X, N, [f], \omega) = \left\{ p : \gamma \rightarrow p(\gamma) = \int_{f_*\gamma} \omega \right\}.$$

The map  $p$  is called the period map of  $\omega$  and it provides coordinates on the space  $\Omega\mathcal{S}_{g,n}$ . Notably, the period coordinates do not allow to recover the differential even on infinitesimal level [17]. Indeed, the isoperiodic deformations define a foliation of  $\Omega\mathcal{S}_{g,n}$  which is called the isoperiodic foliation. Some of the first results on the isoperiodic foliation of holomorphic differentials over the moduli space include that the isoperiodic leaves are Euclidean spaces with complete metric [81]. This work also includes the study of the isoperiodic sets in the holomorphic case with  $g = 2$ . Then, in a fundamental work of Calsamiglia, Derooin, and Francaviglia [17] it was shown that the leaves of the isoperiodic foliation of holomorphic differentials are connected for  $g \geq 2$  and primitive degree at least three. The method used in [17] involves the degeneration of the Riemann surface into a nodal curve which allows to simplify the problem to surfaces of lower genera.

The method proposed in [17] cannot be applied to the meromorphic case because meromorphic differentials can have real periods (i.e., the image  $\text{Im} p$  is contained in  $\mathbb{R}$ ). It is not possible to degenerate a meromorphic form with real periods into a union of forms that includes holomorphic parts because holomorphic forms do not admit real periods (a consequence of Riemann's bilinear relations, [9]). Therefore, the case of real periods of meromorphic forms requires new tools in order to prove connectivity of the isoperiodic sets. In [18] the non-emptiness and connectivity of the isoperiodic leaves in  $\Omega\mathcal{S}_{g,n}$  is shown for meromorphic forms with 2 poles and  $g \geq 1$  of degree at least 3. However, the method of proof relies on the combinatorial properties of having exactly two poles. Our result is the extension of the study of connectivity of the isoperiodic leaves to a higher number of poles in the case of real period. Denote by  $\Sigma_{1,3}$  a surface of genus 1 with 3 marked points:

**Theorem 6.1.4.** Denote by  $\Pi$  the peripheral module of  $\Sigma_{1,3}$ , i.e., a module  $\Pi$  such that  $H_1(\Sigma_{1,3}, \mathbb{Z}) = H_1(\Sigma_1, \mathbb{Z}) + \Pi$ ; let  $p \in \text{Hom}(H_1(\Sigma_{1,3^*}, \mathbb{Z}), \mathbb{C})$  be a

period map. If the image of  $p$  in  $\mathbb{C}$  is real, then the level  $\text{Per}^{-1}(p)$  is connected in  $\Omega\mathcal{S}_{1,3}$  if the image of  $p$  is not contained in the  $\mathbb{Q}$ -vector space generated by  $p(\Pi)$ .

This result is a new step towards proving the connectivity of the isoperiodic sets in general case. The strategy of treating the cases of higher genera and larger number of poles often relies on the degeneration into simpler bits and applying induction. Therefore, the result of Theorem 6.1.4 is meant to serve as a base of induction for our work in progress that studies the connectivity of the leaves of the isoperiodic foliations with real periods. We emphasise that the benefit of the geometrical method used in the present work is that it can be applied to the surfaces of any (small) genus and number of poles unlike the methods used in [18, 59]. However, we believe that the complexity of the proof is growing very fast with larger genus and larger number of poles. To demonstrate the universality of the method for low  $g, n$ , we supplement the proof of Theorem 6.1.4 with Appendix which contains the proof of a similar statement for  $\Sigma_{1,2}$ .

The strategy of the present work relies on applying a local surgery called the Schiffer variation [103]. The Schiffer variation is an isoperiodic surgery of the surface which provides a tool to connect two different forms in  $\Omega\mathcal{S}_{1,3}$  by an isoperiodic path. It is performed by selecting two twins leaving or entering the zero in the same direction with an angle  $2\pi$  between them and making two cuts of the same length along them. Then the sides of the two cuts are re-glued: the left side of the first cut is glued to the right side of the second cut, and vice versa. In this manner the zero can be isoperiodically moved to a different position on the surface.

The main directions of our further study is proving the connectivity of the isoperiodic sets both in real and complex cases for larger genus and number of poles using induction. Another interesting direction of research is to check the ergodicity of the isoperiodic foliation following [17, 18, 48]. An interesting approach of proving ergodicity of a real isoperiodic foliation of forms with a single double pole is proposed in [59] and involves using the cut diagrams.

## 6.2 Rigid forms

In this Section we introduce an important subclass in  $\Omega\mathcal{S}_{1,3}$  of rigid forms, i.e., forms with one zero. We show that any form in  $\Omega\mathcal{S}_{1,3}$  can be connected to a rigid form; therefore, in order to prove Theorem 6.1.4 it suffices to prove the isoperiodic connectedness of the rigid forms. Therefore, it is natural to study possible topological types of the rigid forms.

**Definition 6.2.1** (A rigid form). A rigid form  $(X, N, [f], \omega) \in \Omega\mathcal{S}_{g,n}$  is a form with a single zero. By the Riemann-Roch theorem, the multiplicity of the single zero is equal to  $2g - 2 + n$  and the angle at the zero is  $2\pi(2g - 1 + n)$ .

**Example 6.2.2.** A rigid form in  $\Omega\mathcal{S}_{1,3}$  has a single zero of order 3 with an angle  $8\pi$  around it.

The importance of the subclass of the rigid forms in the context of Theorem 6.1.4 is explained in the following lemma:

**Lemma 6.2.3.** Any form in  $\Omega\mathcal{S}_{1,3}$  with real period map is isoperiodically connected to a rigid form.

*Proof.* A generic form in  $\Omega\mathcal{S}_{1,3}$  has three simple zeroes and the distances between zeroes do not coincide. Let us select two zeroes with the shortest saddle connection between them. This saddle connection has a twin of the same length emerging at an angle  $2\pi$  from one of the two zeroes. If this twin ends at a regular point, performing Schiffer variation along the saddle connection and its twin yields a double zero which is not a node. In the same manner we can connect the double zero to the remaining simple zero, thus, obtaining a rigid form. If the twin described above ends in the same zero, i.e., forms a loop, an infinitesimal perturbation of the form will ensure that it ends at a regular point. Then, the previous argument applies.

If the twin ends at the second zero then the double zero formed by the corresponding Schiffer variation is a node. Note that since the cycle formed by two twins integrates to zero, the node has zero residue. We can show by contradiction that it is a non-separating node. First, it cannot separate the surface into a component with three poles and holomorphic component since holomorphic component does not allow real periods. It also cannot separate one pole from the other two by the residue theorem. We conclude that it is a non-separating node. In this case, we apply the degeneration

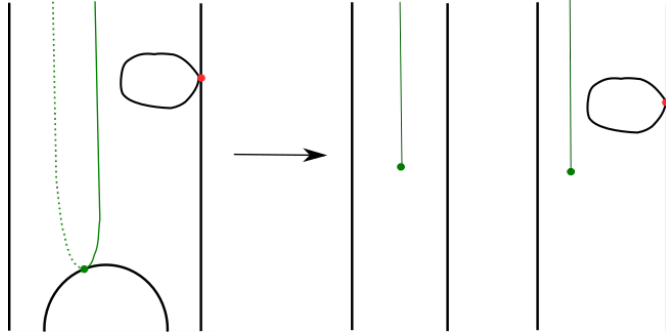


Figure 6.1: A decomposition of the surface  $\Sigma_{1,3}$  with a double zero into a sphere with 2 poles and a torus with 2 poles and a double zero.

technique in order to connect such form to a rigid form.

Let us perform a Schiffer variation along two twins that leave the remaining simple zero in the positive imaginary direction: it results in a decomposition of the initial surface into a sphere with 2 poles and no zeroes and a torus with 2 poles and a double zero which is a node (see Figure 6.1). The toral component can be isoperiodically perturbed into a torus with 2 simple poles and 2 zeroes. In [18] it is shown that a torus with 2 simple poles and 2 zeroes can be isoperiodically deformed into a rigid form with 2 simple poles. In the end, we glue the two parts by selecting a geodesic in the positive imaginary direction emerging from an arbitrary point on the sphere, and a geodesic on the torus leaving the double zero in the positive imaginary direction. We glue the surfaces along these geodesics obtaining a torus with three poles and a single zero of the third order.  $\square$

Lemma 6.2.3 implies that to prove Theorem 6.1.4 it suffices to consider only the rigid forms. Therefore, it is natural to study further the structure and types of the rigid forms in  $\Omega\mathcal{S}_{1,3}$ . We start the discussion with studying the separatrices in real directions that pass through the zero of the rigid form in  $\Omega\mathcal{S}_{1,3}$ .

Select a regular point  $z_0$  on  $\Sigma_{1,3}$  and consider an integral  $f(z) = \int_{z_0}^z \text{Im}\omega$ . Since the periods of  $\omega$  are real the imaginary part of  $\omega$  does not have monodromy, i.e.,  $f$  is a real-valued univalent function  $f: X \rightarrow \mathbb{R}$ . The levels of  $f$  are the leaves of the real foliation on  $X$ . Since residues around each pole are real, one can view poles as semi-infinite annuli where all real leaves are closed and compact manifolds of dimension 1 and no leaf is minimal even

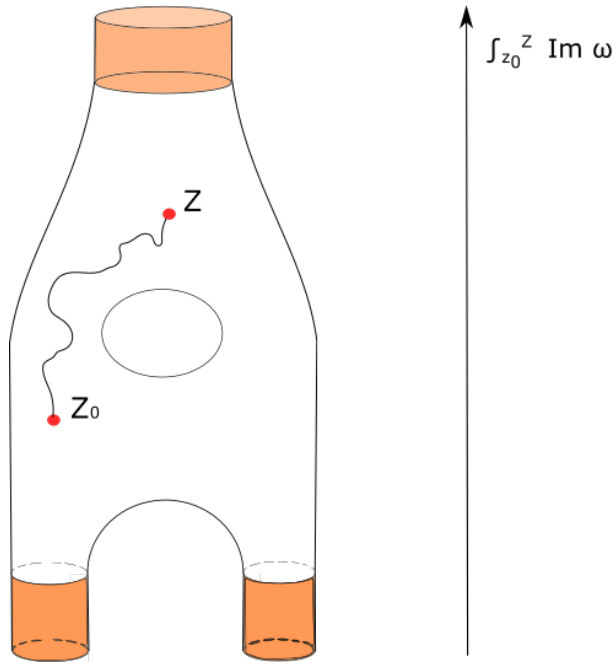


Figure 6.2: Integral  $\int_{z_0}^z \text{Im}(\omega)$  of the imaginary part of a 1-form  $\omega$  defines a function  $f(z)$  on the torus  $X$ . The levels of the function are the leaves of the real foliation of  $\omega$ . These leaves form closed compact 1-dimensional manifolds in the neighbourhood of the poles.

locally (see Figure 6.2). We conclude that any saddle connection leaving a zero in real direction cannot escape to a pole because it cannot transversally cross the leaves of the real foliation. Instead, each saddle connection leaving a zero in real direction has to end in some zero.

It follows for a rigid form in  $\Omega\mathcal{S}_{1,3}$  that all 4 separatrices that leave the zero along real directions come back to the zero along the real directions. Moreover, the outgoing and ingoing real separatrices alternate in order.

### 6.2.1 Octopodes and butterflies

The outgoing separatrices in real directions have to return to the zero; in this subsection we investigate in which order the separatrices return. The order defines the topological type of the rigid form. There are two ways to graphically depict a topological type of a rigid form (see Figure 6.4):

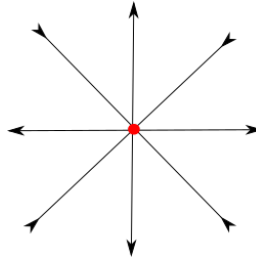


Figure 6.3: The structure of a zero of a rigid form in  $\Omega\mathcal{S}_{1,3}$ : the angle around the zero is  $8\pi$  and in real directions there are 4 outgoing and 4 ingoing separatrices that alternate in order.

- **Radial diagram.** The radial diagram features a zero in its center and the saddle connections leaving the zero and entering the zero. The order in which the in-going and out-going separatrices are connected defines the topological type of the rigid form.
- **Circle diagram.** Both sets of in-going and out-going separatrices in the neighborhood of the zero are presented as two sets of points on a circle. Each out-going point is bijectively connected to an in-going point. The order in which they are connected defines the topological type of the rigid form.

The correspondence between the radial diagrams and the circle diagrams is easy to establish: for the convenience of the reader, we demonstrate it on Figure 6.4. In the Figures hereafter we will be using circle diagrams. It turns out that the order in which the outgoing separatrices enter the zero is not arbitrary, but restricted by the topology of  $\Sigma_{1,3}$  to few options as we see in the following Lemma.

**Lemma 6.2.4.** Up to the change of orientation, there are only 2 possible combinatorial types of rigid forms in  $\Sigma_{1,3}$ .

*Proof.* Each separatrix that leaves the zero of the third order must eventually come back: there are 4 separatrices leaving the zero and 4 entering it. Let us number both sets counter-clockwise from 1 to 4. We need to understand in which order the separatrices that leave the zero come back: it is natural to think about this correspondence as of possible permutations on 4 elements.

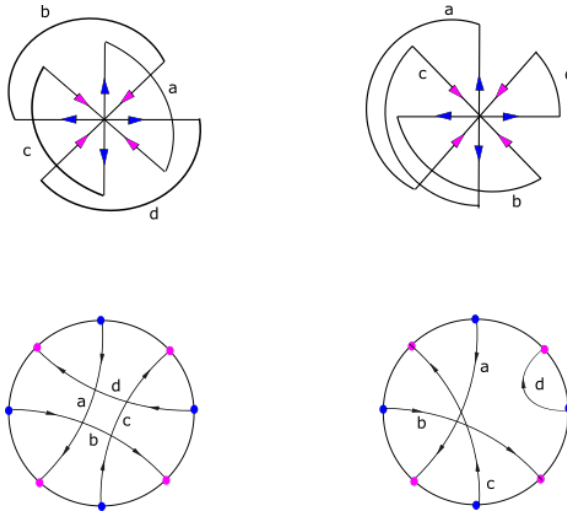


Figure 6.4: Correspondence between the radial (top) and the circle (bottom) diagrams. Left: radial and circle diagrams of the butterflies form, right: radial and circle diagrams of the octopus form.

The geometrical type of the zero does not depend on the rotation of the chosen numbering: therefore, one does not need to consider all possible 24 permutations separately. Instead, it suffices to consider only 10 conjugacy classes by two cyclic permutations (1234) and (1432):

1. constant permutation (1)(2)(3)(4) forms a conjugacy class of 1 element;
2. transpositions of 2 neighboring elements (12)(3)(4)  $\rightarrow$  (23)(4)(1)  $\rightarrow$  (34)(1)(2)  $\rightarrow$  (41)(2)(3) form a class of 4 elements;
3. transpositions of 2 non-neighboring elements (13)(2)(4)  $\rightarrow$  (24)(3)(1) form a class of 2 elements;
4. 2 non-intersecting transpositions of two pairs of neighboring elements (12)(34)  $\rightarrow$  (23)(14) form a class of 2 elements;
5. 2 non-intersecting transpositions of two pairs of non-neighboring elements (13)(24) forms a class of 1 element;
6. three-cycles oriented counterclockwise (123)(4)  $\rightarrow$  (234)(1)  $\rightarrow$  (341)(2)  $\rightarrow$  (412)(3) form a class of 4 elements;

- 
7. three-cycles oriented clockwise  $(132)(4) \rightarrow (243)(1) \rightarrow (314)(2) \rightarrow (421)(3)$  form a class of 4 elements;
  8. four-cycle oriented counterclockwise  $(1234)$  forms a class of 1 element;
  9. four-cycle oriented clockwise  $(1432)$  forms a class of 1 element;
  10. four-cycles with transposition  $(1243) \rightarrow (2314) \rightarrow (3421) \rightarrow (4132)$  form a class of 4 elements.

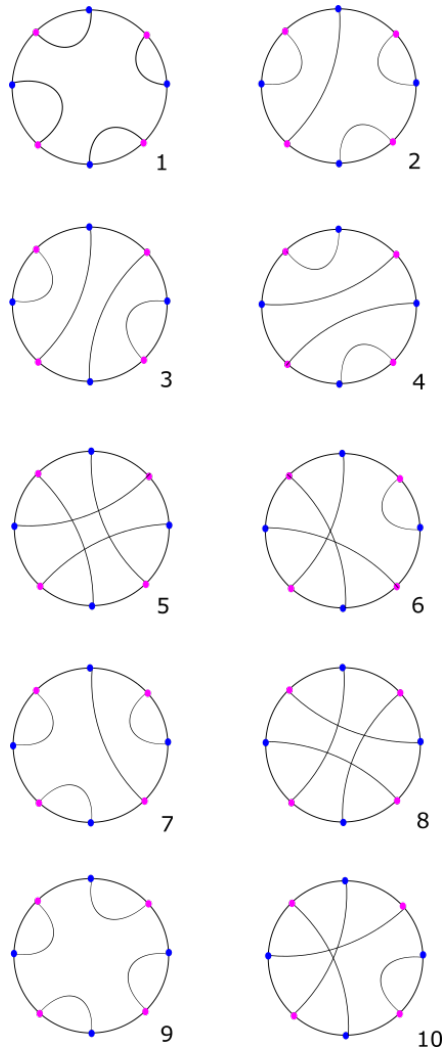


Figure 6.5: Possible combinatorics at a zero of order 3. Figures 1-4, 7,9 correspond to  $g = 0, n = 4$ , Figures 5,6,8,10 correspond to  $g = 1, n = 3$ .

If we cut the surface along the paths following the directions of separatrices on the left hand side and on the right hand side we will obtain the decomposition of the surface into several semi-infinite cylinders. The considered surface  $\Sigma_{1,3}$  can only be decomposed into 3 semi-infinite cylinders because it has three poles. The Figure 6.5 shows that there are only 2 possible combinatorial types where the surface decomposes into 3 semi-infinite cylinders: the first corresponding to cases (5), (8) and the second corresponding to the cases (6), (10). The rest of diagrams represent spheres with 5 punctures.  $\square$

Let us discuss the two topological types of rigid forms more closely. In order to do it we agree on the following conventions and notations:

The surface  $\Sigma_{1,3}$  has three poles whose real residues sum up to zero, so it either has 1 or 2 poles with positive residues. The number of poles with positive residue defines the orientation of the associated form; without loss of generality we assume that all rigid forms have 1 positive pole and 2 negative poles. Then, changing the signs of all residues corresponds merely to switching the orientation of the surface.

Denote the positive pole by  $s_+$  and the two negative poles by  $s_-^<$  and  $s_-^>$  where  $s_-^>$  stands for the negative pole with a residue equal or larger in absolute value than the residue of  $s_-^<$ . Denote the short closed curves going around the poles as  $\pi_+$ ,  $\pi_-^<$  and  $\pi_-^>$ , respectively, and note that  $p(\pi_+) + p(\pi_-^<) + p(\pi_-^>) = 0$  by the residue theorem.

Let us define the two types of the rigid forms:

- **Butterflies** We say that a rigid form associated with marking  $(a, b, c, d)$  is in  $\Omega S_{1,3}$  and is of type "butterflies" if

$$\begin{aligned} & - a \cdot b = b \cdot c = c \cdot d = d \cdot a = 1, a \cdot c = b \cdot d = 0; \\ & - a + c = -\pi_-^>, b + d = -\pi_-^<, a + b + c + d = \pi_+; \\ & - p(a), p(b), p(c), p(d) > 0. \end{aligned}$$

An example of radial and circle diagrams of butterflies is provided on Figure 6.4. For convenience, we denote by  $B(a, c | b, d)$  a butterflies form that satisfies the three conditions listed above.

- **Octopus** We say that a rigid form associated with marking of curves  $(a, b, c, d)$  is in  $\Omega S_{1,3}$  and is of type "octopus" if

- $a \cdot b = b \cdot c = c \cdot a = 1, a \cdot d = b \cdot d = c \cdot d = 0;$
- $a + b + c = -\pi_{-}^{>}, d = -\pi_{-}^{\leq}$     or  
 $a + b + c = -\pi_{-}^{\leq}, d = -\pi_{-}^{>};$
- $a + b + c + d = \pi_{+};$
- $p(a), p(b), p(c), p(d) > 0.$

An example of radial and circle diagrams of octopus is provided on Figure 6.4. Note that the connection  $d$  is distinguished from the other three connections: it is the connection that starts and finishes at adjacent points. We call the connection  $d$  *the head of the octopus*. The head of the octopus generates a closed curve that goes around a pole. By the length considerations, this pole cannot be positive, so it is one of the negative poles (see Figure 6.6). Therefore, there are two distinct cases:  $a + b + c = -\pi_{-}^{>}, d = -\pi_{-}^{\leq}$  and  $a + b + c = -\pi_{-}^{\leq}, d = -\pi_{-}^{>}$ . We call a form associated to the first case *the small head octopus* (SHO) and a form associated to the second case *the large head octopus* (LHO). For convenience, we denote by  $O(a, b, c | d)$  an octopus form that satisfies the three conditions listed above. When the distinction between the large head octopodes and the small head octopodes is important, we use  $LHO(a, b, c | d)$  and  $SHO(a, b, c | d)$ , respectively.

Note that any octopus admits two different orientations and it has to do with the signs of the residues at the three poles (one positive and two negative, or two positive and one negative). However, there is an equivalence between the "left-handed" and "right-handed" octopodes achieved by switching the signs of the residues; hence, there is no necessity to distinguish between these two cases.

### 6.2.2 Schiffer variation on circle diagram.

To perform the Schiffer variation at a zero on the circle diagram we select two neighbouring (i.e., with angle  $2\pi$  in between) separatrices of the same direction and of different lengths. Denote the point corresponding to the shorter separatrix as "Short" and the point corresponding to the longer separatrix as "Long". Denote the shorter separatrix by  $S$  and the longer separatrix by  $L$ . There is a unique separatrix between them that goes in an opposite direction - denote it by  $C$  and the corresponding point by "Central". Perform the Schiffer variation along  $L$  and  $S$  along the whole length of  $S$ : it

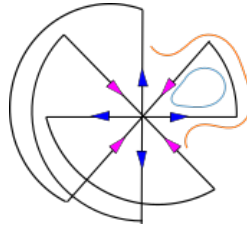


Figure 6.6: The blue curve inside the head of the octopus goes around one of the poles. The blue curve is shorter than the orange curve whose fragment is shown on the Figure. Since  $\pi_+ = \pi_-^< + \pi_-^>$ , the blue curve cannot go around  $n_+$  by the length consideration.

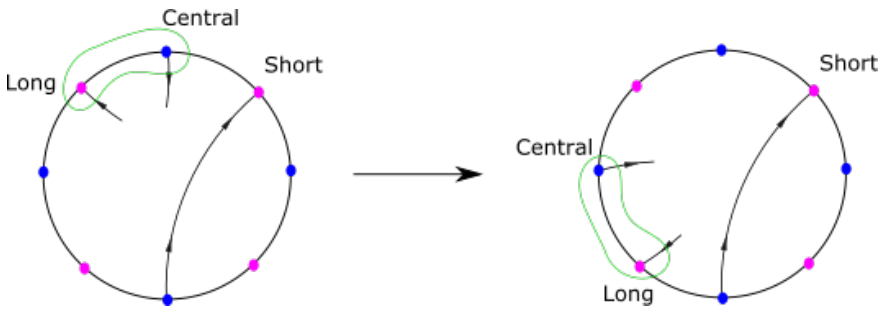


Figure 6.7: The Schiffer variation on a circle diagram: the group  $(L, C)$  of the endpoints of the long and the central connections are "sliding" all the way to the opposite endpoint of the short connection.

yields a new rigid form where the zero is in the same position but the length and order of the saddle connections is changed.

The lengths of the saddle connections will be  $p(L') = p(L) - p(S)$ ,  $p(S') = p(S)$ ,  $p(C') = p(C + S)$ . The positions of the points "Long" and "Central" shift to the opposite end of the short connection  $S$  (see Figure 6.7).

**Remark 6.2.5.** Note that if the two points "Long" and "Central" are the only two points inside the arch of  $S$  then the order of the points does not change.

### 6.2.3 Connecting different types of rigid forms in $\Omega\mathcal{S}_{1,3}$ .

According to Lemma 6.2.4, each rigid form in  $\Omega\mathcal{S}_{1,3}$  is either butterflies or octopus. In this subsection we show how to isoperiodically connect any

rigid form to a large head octopus under mild conditions. The first step is to connect a small head octopus to butterflies and the second step is to connect the butterflies to the large head octopus.

**Lemma 6.2.6.** If the period map of a small head octopus form  $p$  is not contained in the  $\mathbb{Q}$ -vector space generated by  $p(\Pi)$ , it can be connected to a butterflies form.

*Proof.* Consider an octopus  $SHO(a, b, c | d)$ . If  $p(d) > p(c)$  (i.e., if the opposite arm is shorter than the head), then if we perform the Schiffer variation along  $d$  and  $c$  we will reach butterflies in one step. If  $p(d) \leq p(c)$  we treat several cases:

- $p(a)$  and  $p(b)$  are *not rationally dependent*. Without loss of generality, assume  $p(a) > p(b)$ . There are two possible types of Schiffer variations along  $a$  and  $b$ : one changes the order of the marking (namely,  $O(a-b, b, c+b | d)$ ), and the other does not (namely,  $O(b, c+b, a-b | d)$ ). By performing Schiffer variation along  $a$  and  $b$  that does not change the order of the marking we can make  $p(a)$  and  $p(b)$  arbitrarily small while  $p(c)$  grows (similar to Euclidean algorithm). Then, we perform the Schiffer variation along  $a$  and  $b$  that changes the order of arms; depending on their periods, one of them becomes the arm of the octopus which is opposite to the head. The period of the opposite arm is now smaller than the period of the head, therefore, it can be connected to butterflies.
- If  $p(a)$  and  $p(b)$  are *rationally dependent*. All four periods  $p(a), p(b), p(c)$  and  $p(d)$  cannot be rationally dependent because it contradicts the assumption on the image of the period map not being contained in the  $\mathbb{Q}$ -vector space generated by  $p(\Pi)$ . If  $p(c)$  is not rationally dependent with  $p(a)$  we perform a Schiffer variation along  $a$  and  $c$  which does not change the order of the marking. Now the two arms that are not opposite of the head are not rationally dependent: we proceed as in the previous cases. If  $p(c)$  is rationally dependent with  $p(a)$ , then  $p(d)$  is not rationally dependent with any of them. We perform a Schiffer variation along  $c$  and  $d$  which results in an octopus with not all arms rationally dependent. We proceed as in previous cases.

□

**Lemma 6.2.7.** If the image of  $p$  of the butterflies form is not contained in the

$\mathbb{Q}$ -vector space generated by  $p(\Pi)$ , the butterflies form can be connected to a large head octopus form.

*Proof.* Label the butterflies as  $B(a, c | b, d)$  and assume wlog that  $p(a + c) \geq p(b + d)$ . With an appropriate choice of direction, performing a Schiffer variation along neighbouring saddle connections yields an octopus. In this manner one can reach at most 4 different octopodes in one Schiffer variation (see Figure 6.8):

- using saddle connections  $a$  and  $d$ : if  $p(a) < p(d)$ , we can reach an octopus  $O(d - a, b, a | a + c)$  with head  $(a + c)$ , and if  $p(d) < p(a)$ , we can reach an octopus  $O(c, a - d, d | b + d)$  with head  $(b + d)$ ;
- using saddle connections  $a$  and  $b$ : if  $p(a) < p(b)$ , we can reach an octopus  $O(d, b - a, a | a + c)$  with head  $(a + c)$ , and if  $p(b) < p(a)$ , we can reach an octopus  $O(a - b, c, b | b + d)$  with head  $(b + d)$ ;
- using saddle connections  $b$  and  $c$ : if  $p(b) < p(c)$ , we can reach an octopus  $O(a, c - b, b | b + d)$  with head  $(b + d)$ , and if  $p(c) < p(b)$ , we can reach an octopus  $O(b - c, d, c | a + c)$  with head  $(a + c)$ ;
- using saddle connections  $c$  and  $d$ : if  $p(c) < p(d)$ , we can reach an octopus  $O(b, d - c, c | a + c)$  with head  $(a + c)$ , and if  $p(d) < p(c)$ , we can reach an octopus  $O(c - d, a, d | b + d)$  with head  $(b + d)$ .

There are two types of the head that we can obtain in this manner:  $a + c$  and  $b + d$ , which corresponds to the large head octopodes and the small head octopodes. If we are able to reach an octopus with the head  $a + c$ , i.e., a large head octopus, we have confirmed the statement of the lemma. If we are not able to reach a large head octopus, then by the list above it follows that  $p(b), p(d) \leq p(a), p(c)$ . Note that it is not possible that all four pairs  $(p(a), p(b))$ ,  $(p(a), p(d))$ ,  $(p(c), p(b))$ ,  $(p(c), p(d))$  are rationally dependent because it contradicts the assumption of the lemma. Without loss of generality, assume that the pair  $(p(a), p(b))$  is rationally independent.

By assumption,  $p(b) < p(a)$ ; using Schiffer variations along  $a$  and  $b$  several times we can go to another couple of butterflies  $B(a - q \times b, c + q \times b | b, d)$  where  $q \in \mathbb{Z}^+$  is chosen such that  $0 < p(a - q \times b) < p(b)$ . Using the fact that  $p(a - q \times b) < p(b)$ , we use a corresponding Schiffer variation to go to an octopus  $O(d, (q + 1) \times b - a, a - q \times b | a + c)$  which is a large head octopus.  $\square$

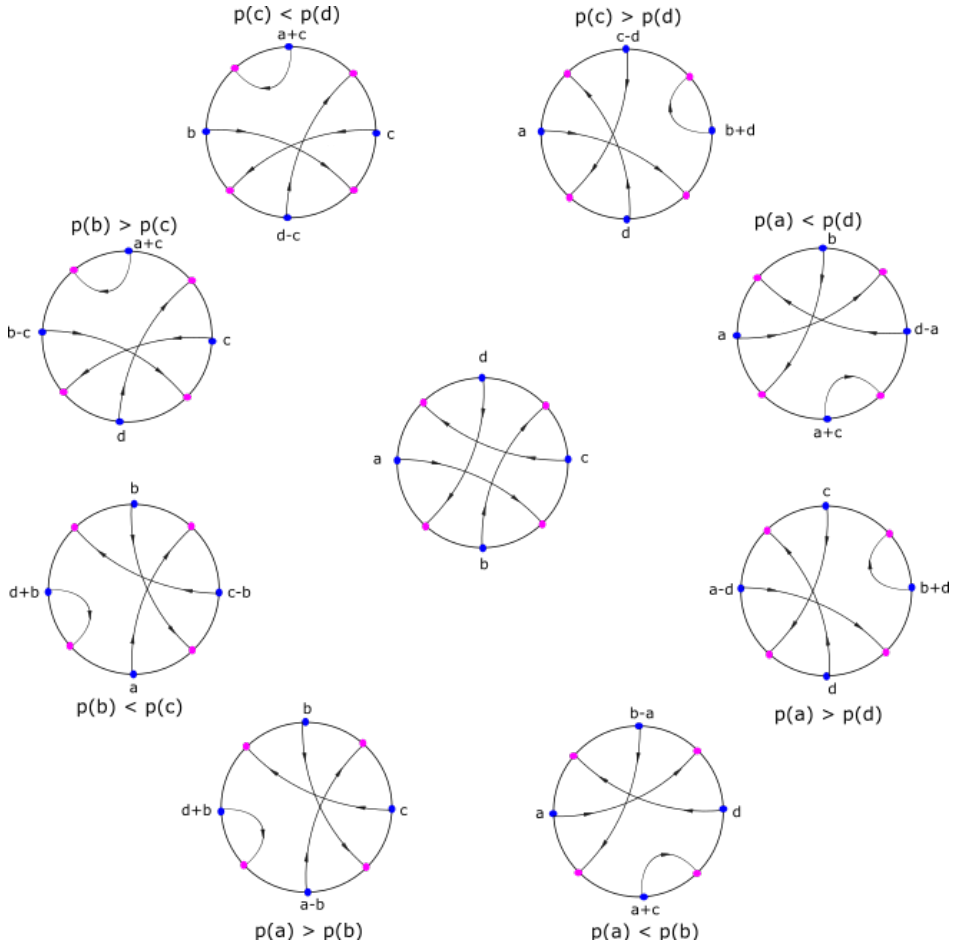


Figure 6.8: Possible octopodes that can be reached from a butterflies form.

---

**Corollary 6.2.8.** To prove Theorem 6.1.4 it suffices to show that any two LHO with same real periods are isoperiodically connected if the image of their period map  $p$  is not contained in  $\mathbb{Q}p(\Pi)$ .

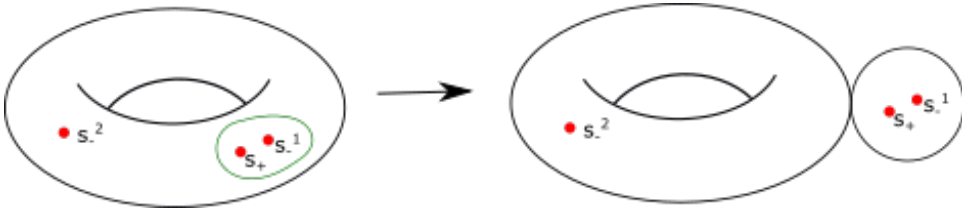


Figure 6.9: Arm module  $M_{s_-^1}$  and the corresponding decomposition of  $\Sigma_{1,3}$ .

## 6.2.4 Arm modules

In order to study the octopodes and the isoperiodic connections between them it is useful to introduce the arm modules. The idea is to degenerate the surface  $\Sigma_{1,3}$  into a nodal stable curve. This degeneration induces a decomposition of the group  $H_1(\Sigma_{1,3}, \mathbb{Z})$ . Select one of the negative poles  $s_-^1$  of  $\Sigma_{1,3}$  and consider a curve that goes around it and the positive pole, does not wind around genus and does not have zeroes and the third pole in its interior. Using Schiffer variation we can degenerate this curve to a node, thus, decomposing  $\Sigma_{1,3}$  into the union of  $\Sigma_{1,s_-^1}$  and  $\Sigma_{0,s_+,s_-^2}$  (see Figure 6.9).

**Definition 6.2.9.** An arm module  $M_{s_-^1}$  associated to a negative pole  $s_-^1$  is a rank 3 submodule of  $H_1(\Sigma_{1,3}, \mathbb{Z})$  such that

$$H_1(\Sigma_{1,3}, \mathbb{Z}) = M_{s_-^1} + \Pi_{s_-^1}, \quad (6.1)$$

where  $M_{s_-^1}$  has rank 3 and  $\Pi_{s_-^1} = \{\pi(s_-^1), \pi(s_+)\}$  has rank 2. The two modules intersect:  $M_{s_-^1} \cap \Pi_{s_-^1} = \mathbb{Z}\pi(s_-^2)$ . The arm module  $M_{s_-^1}$  has a basis  $a, b, c$  where  $p(a), p(b), p(c) > 0$  and  $a \cdot b = b \cdot c = c \cdot a = 1$ . Moreover,  $a + b + c = -\pi_{s_-^2}$ .

The map  $\mu_{s_-^1} : H_1(\Sigma_{1,3}, \mathbb{Z}) \rightarrow H_1(\Sigma_{1,2}, \mathbb{Z})$  restricted to the arm module  $M_{s_-^1}$  is an isomorphism. The form  $p_{M_{s_-^1}} := p \circ \mu_{s_-^1}^{-1} \in \text{Hom}(H_1(\Sigma_{1,2}, \mathbb{Z}), \mathbb{R})$  is called the period of an arm module. Define the quotient arm modules of  $M_{s_-^1}$  and  $M_{s_+}$  as  $M_{s_-^1} / \mathbb{Z}\pi_{s_-^2}$  and  $M_{s_+} / \mathbb{Z}\pi_{s_-^2}$ , respectively. Without loss of generality, let us consider a quotient arm module  $M_{s_-^1} / \mathbb{Z}\pi_{s_-^2}$ : the map  $q : H_1(\Sigma_{1,2}, \mathbb{Z}) \rightarrow H_1(\Sigma_1, \mathbb{Z})$  has  $\pi_{s_-^2}$  in its kernel, and induces an isomorphism between  $M_{s_-^1} / \mathbb{Z}\pi_{s_-^2}$  and  $H_1(\Sigma_1, \mathbb{Z})$ . The reduction  $p_N := p_M \bmod \mathbb{Z}p(\pi_{s_-^2}) \in H^1(\Sigma_1, \mathbb{R} / \mathbb{Z}p(\pi_{s_-^2}))$  is well-defined and called the period of the quotient arm module.

The set of arm modules and the set of quotient arm modules associated to a given pole both have a natural structure of affine space directed by

$H^1(\Sigma_1, \mathbb{Z})$ ; in other words, given two arm modules  $M, M'$  (resp. quotient arm modules  $N, N'$ ) associated to the pole  $s_{\geq}$ , there exists a unique  $\psi \in N^* \simeq H^1(\Sigma_1, \mathbb{Z})$  such that  $M'$  (resp.  $N'$ ) is the image of  $M$  (resp.  $N$ ) by the map  $id|_M + (\psi \circ q) \cdot \pi_{\geq}$  (resp.  $id|_N + \psi \cdot \pi_{\geq}$ ). We will denote  $M' = M + \psi$  and  $N' = N + \psi$  in the sequel.

**Proposition 6.2.10.** To each octopus one can associate an arm module: it is  $M_s$  where  $s$  is the pole associated to the head. Two marked octopodes with the same head and the same arm module can be connected with a finite number of Schiffer variations.

*Proof.* By Figure 6.9 it suffices to appeal to the connectedness of the isoperiodic space of meromorphic forms on a torus with two poles [18], and a convenient attaching map (similar to Lemma 6.2.3 and Figure 6.1).  $\square$

### 6.3 Proof of the connectivity of real isoperiodic sets in $\Omega\mathcal{S}_{1,3}$

This Section contains the proof of Theorem 6.1.4. Proving Theorem 6.1.4 is equivalent to proving Corollary 6.2.8, i.e., proving that the large head octopodes are isoperiodically connected under the conditions of Theorem 6.1.4. We do it in several steps:

1. we show that we can connect  $LHO(a, b, c | d)$  with head  $d$  and arm module  $M = \{a, b, c\}$  to another LHO with arm module  $M + a^*$  where  $a^* \in H^1(\Sigma_1, \mathbb{Z})$  is the dual of  $a$  with respect to the intersection form. In other words,  $a^*(a) = 0, a^*(b) = 1, a^*(c) = -1$  (Lemma 6.3.1);
2. using the previous step, we prove that a LHO with an arm module  $M$  can be connected to a LHO with arm module  $M + \varphi$  if  $p(\varphi^*) \notin \mathbb{Q}/\mathbb{Z}$  (Lemma 6.3.2);
3. we conclude the proof of Corollary 6.2.8 by showing that any two LHO can be connected if the image of the period map is not contained in  $\mathbb{Q}p(\Pi)$  (Lemma 6.3.3).

Let us start with establishing the first step:

**Lemma 6.3.1.** Consider  $LHO(a, b, c | d)$  with an arm module  $M$  generated by  $a, b, c$ . Then there exists a concatenation of a finite number of Schiffer variations that connects this octopus to a LHO with an arm submodule  $M'$  such that  $M' = M + \psi$  with  $\psi = a^*$  where  $a^*$  is defined as  $\text{Ker}(a^*) = a$ .

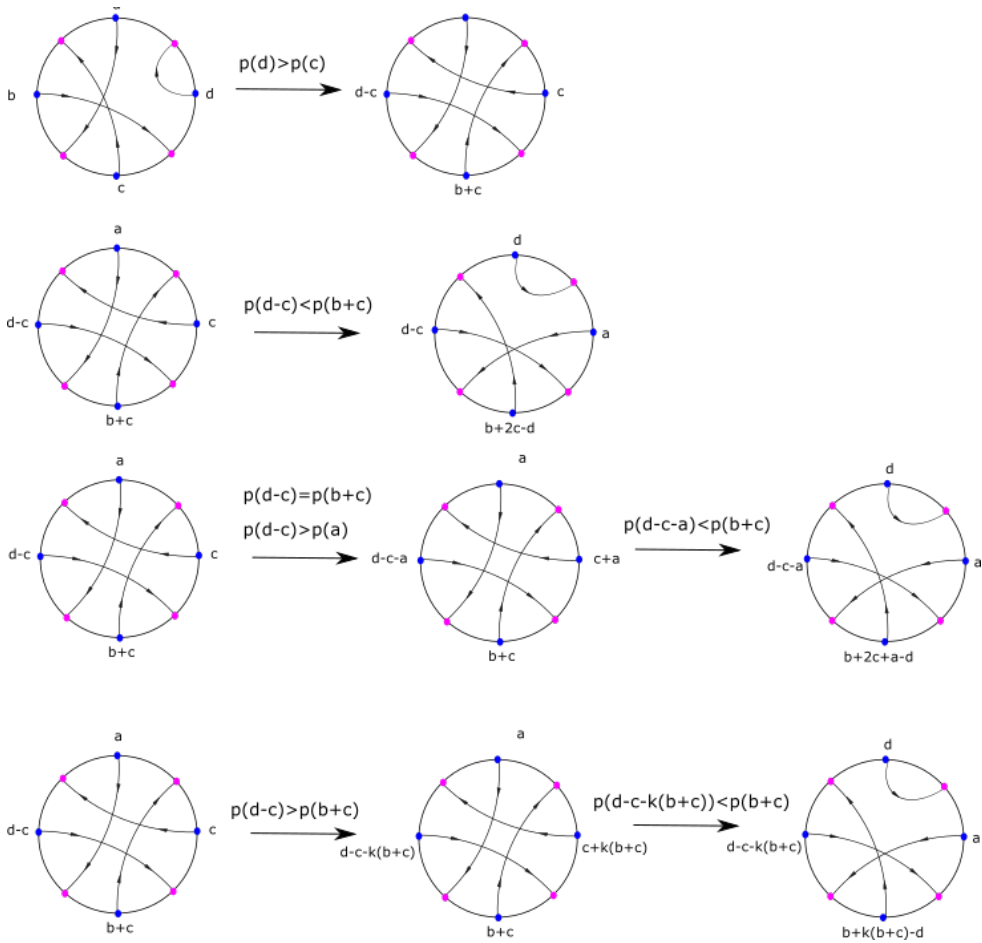


Figure 6.10: Graphical proof of Lemma 6.3.1.

*Proof.* Since the octopus has a large head, let us perform a Schiffer variation along the head  $d$  and the opposite arm  $c$  which will result in butterflies with marking  $B(a, c|d - c, b + c)$ . Consider the cases below - for graphical proof, see Figure 6.10:

1. First, let us consider the case when  $p(d) - p(c) < p(b) + p(c)$ . It follows that we can perform a Schiffer variation along  $d - c$  and  $b + c$  which will result in an octopus with a marking  $O(b + 2c - d, a, d - c | d)$ .
2. Consider the case  $p(d) - p(c) = p(b) + p(c)$ ; since  $p(d) - p(c) > p(a)$ , perform a Schiffer variation along  $a$  and  $d - c$  which results in  $B(a, b + c | d - c - a, c + a)$ . Now  $p(d) - p(c) - p(a) < p(b) + p(c)$  and so we can go to an octopus  $O(b + 2c + a - d, a, d - c - a | d)$ .

3. Now consider that  $p(d) - p(c) > p(b) + p(c)$ . Let us perform  $k$  Schiffer variations that will result in  $B(a, b + c | d - c - k \times (b + c), c + k \times (b + c))$  where  $k \in \mathbb{Z}^+$  is such that  $0 < p(d) - p(c) - k(p(b) + p(c)) < p(b) + p(c)$ . After this we can perform a Schiffer variation along  $d - c - k \times (b + c)$  and  $b + c$ , which will result in an octopus with a marking  $O((k + 1) \times (b + c) + c - d, a, d - c - k \times (b + c) | d)$ .

The octopodes obtained in all three cases have large heads. Observe that in all cases  $\psi = a^*$ . Let us check it in the first case;  $M'$  is generated by  $\{a, d - c, b + 2c - d\}$ . We see that  $\psi(a) = 0$ ,  $\psi(b) = 1$ ,  $\psi(c) = -1$  and, therefore,  $\psi = a^*$ . The other two cases are similar.  $\square$

Two arm modules  $M$  and  $M'$  are connected (denoted by  $M' \sim M$ ) if some LHO with an arm module  $M$  and head  $d$  is connected to some LHO with an arm module  $M'$  and head  $d$ . The connectedness of the set of arm modules implies that each octopus with arm module  $M$  is connected to each octopus with an arm module  $M'$  as we showed in Proposition 6.2.10. In the following lemma's we will be connecting two arm modules which should be understood as finding and connecting two representatives of each module.

**Lemma 6.3.2.** Let  $M, M'$  be arm modules of two large head octopodes and  $M' = M + \psi$ . If  $p_M(\psi^*) \notin \mathbb{Q}/\mathbb{Z}$  then  $M' \sim M$ .

*Proof.* We need to construct an arm basis  $\{a, b, c\}$  of  $M$  which satisfies the following three properties:

1.  $a \bmod \pi_{\geq} = \psi^*$ ;
2.  $a \cdot b = b \cdot c = c \cdot a = 1$ ;
3.  $p(a), p(b), p(c) > 0$ ;

By definition,  $M \bmod \pi_{\leq} = N$ . Taking for simplicity  $p(-\pi_{\leq}) = 1$  we see that  $p_N: N \rightarrow \mathbb{R}/\mathbb{Z}$ . Assume that  $p_N(\psi^*) \notin \mathbb{Q}$  and consider the case when  $\psi^*$  is primitive.

Select  $a_0 = \psi^*$  and  $a = a_0 + k_a \pi_{\geq}$  such that  $p(a) > 0$ . By assumption, the number  $p(a_0)$  is irrational. Select an element  $b_0 \in N$  such that  $a \cdot b_0 = 1$  and select  $k_b$  such that  $p(b_0 + k_b \pi_{\geq}) > 0$ . Note that  $a \cdot (b_0 + k_b \pi_{\geq}) = 1$  since  $\pi_{\geq} \cdot a = 0$ .

If  $p(a) + p(b_0 + k_b\pi^{\geq}) < 1$  then we can uniquely choose the last element  $c$  such that  $p(c) = 1 - p(a) - p(b_0 + k_b\pi^{\geq})$ . If  $p(a) + p(b_0 + k_b\pi^{\geq}) > 1$  introduce a constant  $\bar{k}_b$  such that  $0 < p(b_0 + k_b\pi^{\geq} + \bar{k}_b a_0) < 1 - p(a)$  (denote  $b_0 + k_b\pi^{\geq} + \bar{k}_b a_0$  by  $b$ ). This is possible since  $p(a_0)$  is irrational by assumption. Note that  $a \cdot b = 1$ . Now the reasoning follows the case  $p(a) + p(b_0 + k_b\pi^{\geq}) < 1$ .

By Lemma 6.3.1 we can connect the LHO with the arm module  $a, b, c$  that we constructed above to a LHO with an arm module  $M'$  such that  $M' = M + \psi = M + a^*$  which concludes the proof for primitive  $\psi^*$ . If  $\psi^*$  is not primitive, we can connect  $M$  and  $M' = M + \psi$  in several similar steps, but for this we require that  $p(\psi^*)$  is irrational.  $\square$

**Lemma 6.3.3.** Any two arm modules  $M$  and  $M'$  associated to the same pole are connected if the image of the period map is not contained in the rational space  $\mathbb{Q}\Pi$  generated by the peripheral periods.

*Proof.* Assume that  $M' = M + \psi$ . If  $p_M(\psi^*) \notin \mathbb{Q}/\mathbb{Z}$ , then, by Lemma 6.3.2,  $M$  is connected to  $M'$ , and the proof is complete. If  $p_M(\psi^*) \in \mathbb{Q}/\mathbb{Z}$ , we construct an auxiliary arm module  $M''$  such that  $M \sim M''$  and  $M'' \sim M'$ .

Note that the auxiliary arm module  $M''$  is completely defined by  $\varphi$  where  $M'' = M' + \varphi$ ; in this case,  $M'' = M + \varphi + \psi$ . It follows that we need to find  $\varphi$  such that  $p_{N'}(\varphi^*)$  is irrational and  $p_N(\varphi^* + \psi^*)$  is irrational; then, by the previous Lemma,  $M \sim M'' \sim M'$ .

Fix a basis  $\{x, y\}$  of  $H_1(\Sigma_1, \mathbb{Z})$ : then, in this basis the element  $\varphi^* \in H_1(\Sigma_1, \mathbb{Z})$  is given by a pair  $(n_x x, n_y y)$ ,  $n_x, n_y \in \mathbb{Z}$ . Then,  $p_N(\varphi^*) = n_x \alpha + n_y \beta$  where  $\alpha = p_N(x) \in \mathbb{R}/\mathbb{Z}$ ,  $\beta = p_N(y) \in \mathbb{R}/\mathbb{Z}$ , and by the assumptions of the lemma  $\alpha \notin \mathbb{Q}\Pi$  or  $\beta \notin \mathbb{Q}\Pi$ . By the linearity,  $p_{N'}(\varphi^*) = p_N(\varphi) + \psi(\varphi^*)p(d)$ . Note that  $\psi(\varphi^*)p(d) \in \mathbb{Z}p(d)$ ; so,  $p_{N'}(\varphi^*) \notin (\mathbb{Q} + \mathbb{Q}p(d))/\mathbb{Z}$  is equivalent to  $p_N(\varphi^*) \notin (\mathbb{Q} + \mathbb{Q}p(d))/\mathbb{Z}$ . Additionally, take  $p_N(\psi^*) = \gamma \in \mathbb{R}/\mathbb{Z}$ . Then, we need to find  $n_x, n_y \in \mathbb{Z}$  such that

$$p_N(\varphi^* + \psi^*) = n_x \alpha + n_y \beta + \gamma \notin (\mathbb{Q} + \mathbb{Q}p(d))/\mathbb{Z} \quad \text{and}$$

$$p_N(\varphi^*) = n_x \alpha + n_y \beta \notin (\mathbb{Q} + \mathbb{Q}p(d))/\mathbb{Z}.$$

Denote the space  $(\mathbb{Q} + \mathbb{Q}p(d))/\mathbb{Z}$  by  $Q$ . Select arbitrary  $(n'_x, n'_y) \in \mathbb{Z}^2$ ; if  $\alpha n'_x + \beta n'_y \notin Q$  we fix this selection  $(n_x, n_y) = (n'_x, n'_y)$ . If  $\alpha n'_x + \beta n'_y \in Q$  then  $\alpha(n'_x + 1) + \beta n'_y \notin Q$  since either  $\alpha \notin Q$  or  $\beta \notin Q$ , so, wlog, we assume it for  $\alpha$ . Then, we fix the selection  $(n_x, n_y) = (n'_x + 1, n'_y)$ . If  $\alpha n_x + \beta n_y + \gamma \notin Q$  then we found  $(n_x, n_y)$  that satisfy the conditions above and we are done. If  $\alpha n_x + \beta n_y + \gamma \in Q$  we conclude that  $\alpha 2n_x + \beta 2n_y + \gamma \notin Q$  because  $\alpha n_x + \beta n_y \notin Q$  by construction. Then,  $(2n_x, 2n_y)$  satisfy the conditions above and we are done.  $\square$

Lemma 6.3.3 sums up the proof of Theorem 6.1.4.

## 6.4 Appendix: connectivity of real isoperiodic sets in $\Omega\mathcal{S}_{1,2}$

In this Section we show that the level  $\text{Per}^{-1}(p)$  is connected in  $\Omega\mathcal{S}_{1,2}$  if the image of  $p$  is contained in  $\mathbb{R}$ . A simple argument can be found in Section 3 of [18]; here, we present a lengthier geometrical argument which inspired the geometrical proof of Theorem 6.1.4. Using the notation proposed in the introduction we formulate the following proposition:

**Proposition 6.4.1.** The level  $\text{Per}^{-1}(p)$  is connected in  $\Omega\mathcal{S}_{1,2}$  if the image of  $p$  is real.

Consider a torus  $\Sigma_{1,2}$  equipped with a meromorphic differential  $\omega$  having two simple poles  $s_+$  and  $s_-$ . Let us denote by  $X^*$  the torus with punctures at  $s_+$  and  $s_-$  and consider a marking of  $X^*$ , i. e., a basis  $m \in H_1(X^*, \mathbb{Z})$ . As  $X$  is compact, the sum of the residues around the poles is equal to zero by the residue theorem. The basis  $m$  has three components  $a, b, c$  such that  $a + b + c = \pi_+$ , where  $\pi_+$  is a curve going around a marked "positive" pole  $s_+$  (the choice of a "positive" and a "negative" pole is included in the marking).

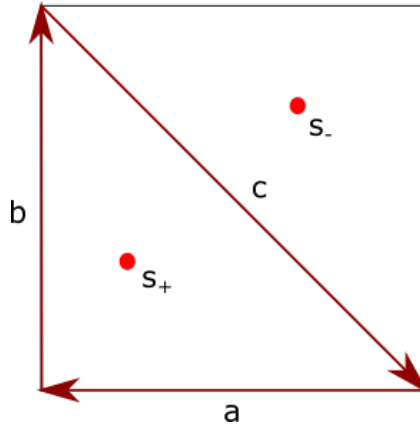
Let us equip the group  $H_1(X^*, \mathbb{Z})$  with a standard intersection form  $(\cdot)$  such that  $a \cdot b = b \cdot c = c \cdot a = 1$ . Then, it is easy to check that  $\pi_+$  belongs to the kernel of the intersection form. Moreover,  $\text{Ker}(\cdot) = \mathbb{Z}\pi_+$ . Fix three real numbers  $(\alpha, \beta, \gamma) \in \mathbb{R}^3$  as the real period coordinates and consider  $M_{(\alpha, \beta, \gamma)}$  - the Torelli space of marked meromorphic differentials  $(X^*, \omega, a, b, c)$  with

$$p(a) = \alpha, p(b) = \beta, p(c) = \gamma.$$

Note that

$$\text{res}_{s_+} = \alpha + \beta + \gamma \neq 0,$$

because  $s_+$  is a simple pole of  $\omega$  (see Figure 6.11). Without loss of generality we can assume that  $\text{res}_{s_+} = 1$  and  $\text{res}_{s_-} = -1$ . The form  $\omega$  that has 2 poles also has two zeroes by the Riemann-Roch theorem. Assume that  $\text{Im}(\int_{z_2}^{z_1} \omega)$  is not zero: let us perform the Schiffer variations until  $\text{Im}(\int_{z_2}^{z_1} \omega) = 0$ . It can happen that after this operation the two zeroes coincide forming a zero of order two. In this case is easy to see that

Figure 6.11: A marking on  $\Sigma_{1,2}$ .

**Lemma 6.4.2.** A zero of order two of a meromorphic differential with two poles on a torus has a unique topological type.

*Proof.* The proof is similar to the proof of Lemma 6.2.4, therefore, we provide a short version here. Each separatrix that leaves the double zero in a real direction has to come back along a real direction. Therefore, we have to consider the three different orders (up to rotation) in which the three outgoing separatrices come back (see Figure 6.12). Note that cutting the surface along the left and the right directions along separatrices decomposes the surface  $\Sigma_{1,2}$  into a union of semi-infinite cylinders. Since the number of poles is 2, the number of semi-infinite cylinders is also 2. We see that the types 1 and 2 on Figure 6.12 are therefore not possible; the only possible combinatorics is type 3 on Figure 6.12.  $\square$

Let us fix a marking  $m = (a, b, c)$  of  $H_1(\Sigma_{1,2}, \mathbb{Z})$ . Any other marking  $m' = (a', b', c')$  differs from  $m = (a, b, c)$  by an automorphism of  $(H_1(X^*, \mathbb{Z}), \cdot, \pi_+)$ , i. e., by a positively oriented automorphism of the first homology group preserving the intersection form and both cycles  $\pi_+$  and  $\pi_-$ . Therefore, the set of markings is  $\text{Aut}(H_1(X^*, \mathbb{Z}), \cdot, \pi_+)$ .

**Lemma 6.4.3.** The family of automorphisms gives rise to a short exact sequence:

$$0 \rightarrow \mathbb{Z}^2 \rightarrow \text{Aut}(H_1(X^*, \mathbb{Z}), \cdot, \pi_+) \rightarrow \text{Aut}(H_1(X^*, \mathbb{Z})/\text{Ker}(\cdot, \cdot)) \rightarrow 0$$

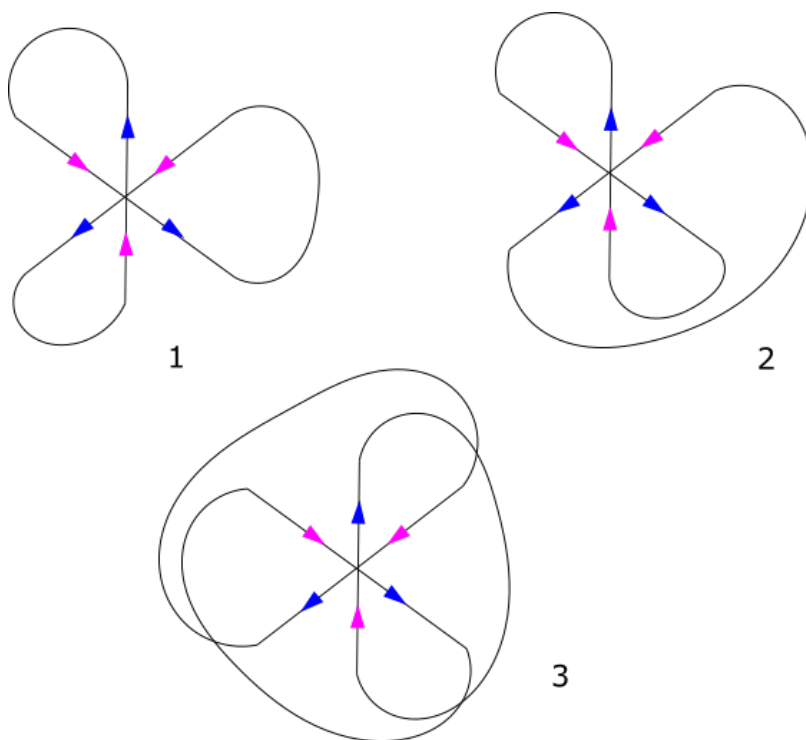


Figure 6.12: Possible combinatorics of a double zero on  $\Sigma_{1,2}$ . Since the number of poles is 2, types 1 and 2 are not possible, and type 3 is the only possible combinatorics.

The group  $\text{Ker}(\cdot)$  is a free  $\mathbb{Z}$ -module of rank 2 over the set of markings and, hence, its action is isomorphic to  $\mathbb{Z}^2$ . Therefore,  $\text{Aut}(H_1(X^*, \mathbb{Z})/\text{Ker}(\cdot), \cdot)$  is isomorphic to the group  $\text{SL}(2, \mathbb{Z})$ .

*Proof.* The sum of any triple of periods  $\alpha' + \beta' + \gamma'$  is fixed to be equal to 1 because of the normalization. As the intersection form is preserved and its kernel is generated by  $\pi_+$ , for any other marking  $(a', b', c')$  it holds that  $a' = a + q\pi_+$ , and  $b' = b + r\pi_+$ . Then,  $c'$  is determined to be  $c - (q + r)\pi_+$  to satisfy the sum condition. Therefore, any element in the kernel of the action of  $\text{Ker}(\cdot)$  on the markings is determined by a pair of integers  $q, r$ . Vice versa, any  $q, r \in \mathbb{Z}$  define an element  $f_{(q,r)} \in \text{Ker}^2(\cdot)$  that sends a triple  $(a, b, c)$  to a triple  $(a + q\pi_+, b + r\pi_+, c - (q + r)\pi_+)$ . The defined map is an isomorphism. Therefore, the action of  $\text{Ker}(\cdot)$  on the set of markings is isomorphic to  $\mathbb{Z}^2$ . It follows that a group of automorphisms  $\text{Aut}(H_1(X^*, \mathbb{Z})/\text{Ker}(\cdot), \cdot)$  is isomorphic to  $\text{SL}(2, \mathbb{Z})$ . It acts as a matrix on the first two entries  $a$  and  $b$  of the marking; the third entry is defined via the sum condition.  $\square$

**Lemma 6.4.4.** Let us call a marking  $(a', b', c')$  positive if  $p(a), p(b), p(c) > 0$  and their sum is equal to 1. There is a bijection between the set of positive markings and a group  $\text{PSL}(2, \mathbb{Z})/\mathbb{Z}_3$ . Since the Cayley graph of  $\text{PSL}(2, \mathbb{Z})/\mathbb{Z}_3$  with generators  $z \rightarrow \pm 1$  and  $z \rightarrow \frac{z}{z+1}$  is connected we conclude that the isoperiodic foliation is also connected.

We start the proof by claiming that there is a bijection between the set of the surfaces with a double zero and the positive markings up to a cyclic permutation. Indeed, every meromorphic differential  $\omega$  with two simple poles and a double zero on a torus injectively corresponds to a positive marking (without loss of generality, we can assume that the periods are positive for every meromorphic differential).

To prove the second inclusion, let us construct a 1-form  $\omega$  given a positive marking  $(\alpha', \beta', \gamma')$ . The marking determines the three loops at the double zero and their ordering. Therefore, it determines  $\pi_+$  and  $\pi_-$  in the neighborhood of the loops. Take two semi-infinite cylinders  $C_1$  and  $C_2$  both with the circular circumference of length 1. Glue the circular boundary of  $C_1$  to  $\pi_+$  and the circular boundary of  $C_2$  to  $\pi_-$ . The resulting surface is a torus with two poles and marking  $(\alpha', \beta', \gamma')$ . We conclude the bijection between the set of positive markings and a factor of  $\text{PSL}(2, \mathbb{Z})$  with respect to  $\mathbb{Z}_3$ .

Fix a marking  $(a, b, c)$  in  $H_1(X^*/\text{Ker}(\cdot), \cdot)$  and act on it with  $\text{PSL}(2, \mathbb{Z})$ . We claim that in each fiber of this action there is a unique positive marking. Let

$(a', b', c')$  be an image of  $(a, b, c)$  under an action of an element of  $\mathrm{PSL}(2, \mathbb{Z})$ . Pass to a triple of lengths  $(\alpha', \beta', \gamma')$  and take their positive fractional parts, arriving to a triple  $([\alpha'], [\beta'], [\gamma'])$  (since  $\pi_+ = 1$  is in  $\mathrm{Ker}(\cdot)$ ). It is clear that the sum of the fractional parts is an integer; therefore, it is either 1 or 2. If it is 1, then this marking is positive and it satisfies the sum condition; therefore, it belongs to the image of  $\mathrm{PSL}(2, \mathbb{Z})$ . If the sum is 2, take  $([\alpha'] - 1, [\beta'] - 1, [\gamma'] - 1)$ . For  $\mathrm{PSL}(2, \mathbb{Z})$  it is equivalent to  $(1 - [\alpha'], 1 - [\beta'], 1 - [\gamma'])$ , which is then a positive marking satisfying the sum condition; therefore, it belongs to the image of  $\mathrm{PSL}(2, \mathbb{Z})$ . Vice versa, every positive marking lies in the image of  $\mathrm{PSL}(2, \mathbb{Z})$  due to the short exact sequence.

Let us construct a graph  $\mathfrak{G}$  representing the surfaces for which  $\mathrm{Im}(\int_{z_2}^{z_1} \omega) = 0$ . This graph is a retraction of the Torelli space to the subspace given by the condition  $\mathrm{Im}(\int_{z_2}^{z_1} \omega) = 0$ . The vertices of the graph are the surfaces having a double zero. Two vertices are connected with an edge if one can be transformed into another using the Schiffer variation in one step keeping the condition  $\mathrm{Im}(\int_{z_2}^{z_1} \omega) = 0$ . Next step is to show that each vertex of the graph belongs to three edges.

Indeed, without loss of generality, assume that  $\alpha < \beta < \gamma$ . Then, to conserve the positivity of the triple, one can only obtain three other triples with a single Schiffer variation, namely,  $(\alpha, \beta - \alpha, \gamma + \alpha)$ ,  $(\alpha, \beta + \alpha, \gamma - \alpha)$ , and  $(\alpha + \beta, \beta, \gamma - \beta)$ . The corresponding markings are  $(a, b - a, c + a)$ ,  $(a, b + a, c - a)$ , and  $(a + b, b, c - b)$ . As the transformations are reversible, the graph is not oriented. It follows that the graph  $\mathfrak{G}$  is a three-valent graph; moreover, we continue to show that there is a bijection between its set of vertices and  $\mathrm{PSL}(2, \mathbb{Z})/\mathbb{Z}_3$ . We show that the graph  $\mathfrak{G}$  is connected; therefore, the corresponding isoperiodic set is also connected.

To see it, take a standard fundamental domain of  $\mathrm{PSL}(2, \mathbb{Z})$  on the upper half plane. Acting on it with  $\mathrm{PSL}(2, \mathbb{Z})$  we cover the whole upper half plane with the images of the standard fundamental domain. Consider the boundary of this covering as a graph  $\mathfrak{G}'$  ignoring the edges that go to infinity on the upper half-plane (i.e., vertical edges going upwards to infinity and the edges reaching the bottom line).

Take a point  $e^{i\pi/3}$  which is a vertex of  $\mathfrak{G}'$ . It is easy to see that the three vertices connected to  $e^{i\pi/3}$  are the images of  $e^{i\pi/3}$  under the transformations  $z \rightarrow \pm 1$  and  $z \rightarrow \frac{z}{z+1}$ . As the graph  $\mathfrak{G}'$  is transitive with respect to the group  $\mathrm{PSL}(2, \mathbb{Z})$ , this holds for every vertex and its three neighbours. However, the

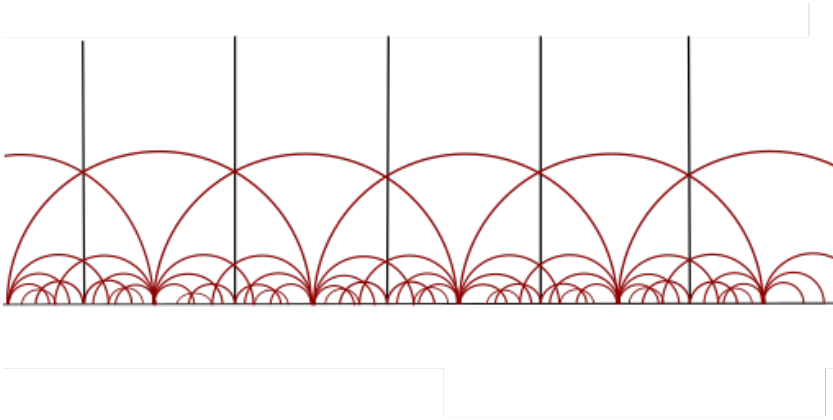


Figure 6.13: Fundamental domains of  $\mathrm{PSL}(2, \mathbb{Z})$  covering the upper half plane

same thing holds for the graph  $\mathfrak{G}$ : as the order in the triple is not relevant, reorder it so that  $\alpha < \beta < \gamma$ . Then, the allowed moves from the triple  $(a, b, c)$  are:  $(a, b - a, c + a)$ ,  $(a, b + a, c - a)$ ,  $(a + b, b, c - b)$ . If we restrict ourselves to the first two entries, we have  $(a, b) \rightarrow (a, b + a)$ ,  $(a, b - a)$ ,  $(a + b, b)$ , which, in  $\mathrm{PSL}(2, \mathbb{Z})$  correspond to  $z \rightarrow \pm 1$  and  $z \rightarrow \frac{z}{z+1}$ . Therefore,  $\mathfrak{G}'$  and  $\mathfrak{G}$  are the same graph. As  $\mathfrak{G}'$  is connected, so is  $\mathfrak{G}$ . This concludes the proof of the connectivity of the isoperiodic foliation of  $\Sigma_{1,2}$ .